Plasma Physics and Controlled Fusion, Vol. 32, No. 11, pp. 903 to 916, 1990.
Printed in Great Britain.

0741-3335/90 $3.00 + .00
IOP Publishing Ltd. and Pergamon Press plc.

TRANSPORT AND FLUCTUATIONS IN REVERSED FIELD PINCHES

S.C. Prager

University of Wisconsin
Madison, Wisconsin USA

ABSTRACT

In the reversed field pinch various turbulent transport mechanisms might be simultaneously active, including MHD flow effects, free-streaming in a stochastic magnetic field, direct transfer of fluctuating energy to ions, and electrostatic fluctuation driven transport. By comparing fluctuations and transport in the RFP to that in the related toroidal configurations of the tokamak and stellarator, a greater understanding of toroidal confinement in general might be achieved. In addition to particle and energy transport, current tranport sustains the reversed field magnetic configuration and constitutes the dynamo effect. Recent results are available from RFP experiments on electrostatic fluctuations, anomalous ion heating, the presence of free-streaming fast electrons, and the extension of these effects to plasmas of large size. The reactor promise of the RFP is based upon the conjecture that the beta value will remain high and the resistance scaling classical, as has been the case in past experiments. One might expect beta to be limited by resistive interchange turbulence. The MST, RFX, and ZTH experiments will form a sequence of devices to test this scaling conjecture to large size and large current values.

KEYWORDS

Reversed field pinch; turbulence; transport; dynamo; magnetic fluctuations; electrostatic fluctuations

INTRODUCTION

In the reversed field pinch (RFP), plasma fluctuations and equilibrium profiles are coupled. Fluctuations are determined by the spatial profiles of the equilibrium quantities (obtained after averaging over the faster spatial and temporal scales of the fluctuations). The equilibrium quantities are in turn determined through fluctuation-induced transport. Such a self-consistent picture applies to the transport of particles and energy in other confinement configurations as well. In the RFP the current density profile is also believed to be determined by transport (of current) from fluctuations. This current transport constitutes a self-generation of a portion of the magnetic field, a well-known effect referred to as the dynamo. The magnetic fluctuations in an RFP are relatively large and turbulent. Thus, the magnetic fluctuations and dynamo in the RFP have functioned as a model problem of fluctuation-induced transport. Indeed, an elegant MHD model has been developed for the sustainment of the RFP magnetic field configuration by tearing mode fluctuations. Features of measured edge magnetic fluctuations are compatible with tearing modes. It is generally believed that magnetic fluctuations also dominate energy transport. However, experimental validation of magnetic fluctuation driven transport of either current or energy is lacking. In addition, the effect of electrostatic fluctuations (e.g., in density and electric potential) is only now beginning to be carefully attacked experimentally in the edge of the

RFP. Thus, the RFP remains an excellent vehicle to test various theories of fluctuations and transport. In this report we illustrate the status of the subject through recent results.

There are at least two reasons for pursuing RFP research. The first is its potential as a fusion reactor. Interest in the RFP reactor stems from its low toroidal magnetic field which leads to a high beta, compact, high power density reactor concept with normal, not superconducting, field coils. The reactor promise of the RFP depends greatly on confinement at large plasma current. A well-coordinated experimental program is in place to test confinement in a sequence of devices existing and now under construction. The second reason for RFP research is its contributions to the understanding of toroidal confinement in general. The physics of the RFP is closely connected to that of the tokamak and stellarator. For example, both the tokamak and RFP are axisymmetric current-carrying tori with helical magnetic field. In principle, if the toroidal magnetic field of a tokamak is reduced to the magnitude of the poloidal field, the plasma will spontaneously relax to an RFP. Most experimental and theoretical techniques are readily transferable between these three confinement concepts. It is highly useful to compare plasma turbulence and transport in these toroidal configurations, which are presently under study worldwide.

Turbulence is presumably determined by gradients within the plasma, by intensive parameters, and by geometric properties of the magnetic field. The gradients of relevant quantities (such as density, temperature, current density and resistivity) are roughly similar in all three toroidal concepts. The relevant intensive parameters (such as gyroradii and collisionless skin depth) are also roughly similar in all three concepts. However, the properties of the magnetic field differ. In Table I we describe the RFP by comparing its geometric properties with that of the tokamak and stellarator. The average curvature in the tokamak is good (for $q > 1$), for a stellarator it can be either good or bad, and for an RFP it is bad (since the poloidal field is dominant, i.e., the safety factor q is less than unity). The local curvature in both the tokamak and stellarator varies from good to bad along a magnetic surface, but is roughly uniform in an RFP. The effect of the bad curvature in the RFP is compensated by the high magnetic shear, which provides stability to ideal interchange modes. In the RFP the magnetic shear is high (the shear length, L_s, is about equal to the minor radius, with q decreasing with radius, $dq/dr < 0$), while in the tokamak the shear is medium (with $L_s \approx R$, the major radius, and $dq/dr > 0$), and in the stellarator the shear is variable from medium ($L_s \approx R$, $dq/dr < 0$) to zero. The magnetic field inhomogeneity along a magnetic surface determines the trapped particle fraction and the importance of neoclassical effects. The trapped particle fraction is high in the tokamak

Table I. Comparison of magnetic field properties of different toroidal configurations

	Tokamak	Stellarator	RFP
Average curvature	Good (for $q > 1$)	Good or Bad	Bad
Local curvature	Good & Bad	Good & Bad	Bad
Shear	Medium ($L_s \approx R$, $dq/dr > 0$)	Medium to zero ($dq/dr < 0$)	High ($L_s \approx a$, $dq/dr < 0$)
Trapped Particle Fraction	High ($\approx\sqrt{2\varepsilon}$)	low or high	low
Dimensionality (of mean field)	2D	3D	2D (toroidicity weak)
Current density (j/B)	medium	low	high

($\approx (2\varepsilon)^{1/2}$ where ε is the inverse aspect ratio), is low in the RFP and is variable in Particle and energy transport in the RFP have traditionally been the stellarator. The mean field in the stellarator is three-dimensional, and is two-dimensional in the axisymmetric tokamak and RFP (which for some phenomena, the weak poloidal asymmetry renders essentially one-dimensional). Finally, the current density (normalized, for example, to the toroidal magnetic field) varies from high in the RFP to medium in the tokamak to nearly zero in the stellarator. Thus, we see that the three configurations span a wide spectrum in important geometric parameters. Comparing the fluctuations and transport between the different concepts affords a controlled variation of parameters not accessible in a single device.

The geometric properties imply which turbulence models might be relevant to each configuration. For example, consider the contributions from interchange, drift wave, tearing, and rippling flucutations. Pressure-driven resistive interchange modes might be dominant in the current-free stellarator and in the outer confinement zone of the RFP. In the tokamak, at high beta, resistive interchange turbulence is expected to be important, modified as resistive ballooning modes with slightly varying amplitude along a magnetic surface. Drift wave fluctuations are ubiquitous. The current-driven tearing modes are a major factor in tokamak and RFP behavior. Current-driven rippling (resistivity-gradient-driven) modes are considered for edge turbulence in the tokamak, but have not yet been addressed in the RFP. The current-free stellarator avoids both tearing and rippling modes.

The experimental program to investigate RFP transport phenomena encompasses the well-studied existing devices (such as ZT40M at Los Alamos, HBTX at Culham, Eta Beta II at Padua, REPUTE at Tokyo, and TPE-1RM15 at Tsukuba), the new MST experiment at Wisconsin, and the two devices under construction, RFX at Padua and ZTH at Los Alamos. Figure 1 illustrates the growth in size of the experiments with MST, RFX, and ZTH being of somewhat comparable size with minor radii about twice

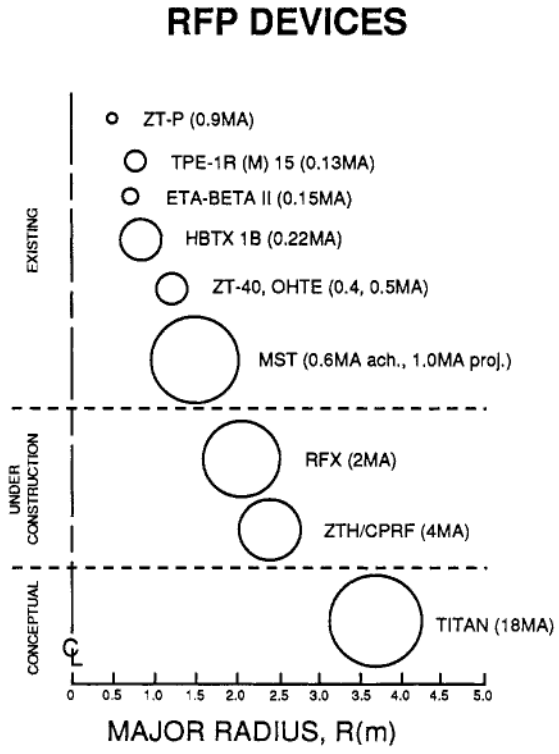

Fig. 1. Comparison of sizes of existing and planned RFP devices.

that of other existing devices. The RFP reactor is represented by the Titan compact reactor design. The device progression will extend the plasma current substantially, from past devices at typically several hundred kiloamperes to MST at 0.6 MA presently (with perhaps 1 MA achievable), to RFX at 2 MA and ZTH at 2-4 MA. The RFX and ZTH experiments will determine whether the RFP should be carried to the next stage in reactor development.

TRANSPORT FLUXES

RFP behavior is determined by the transport of particles, energy, and field-aligned current. Each transported quantity, if fluctuation-driven, is related to a product of fluctuating quantities. To distinguish various transport mechanisms ultimately requires an experimental measurement of the quadratic quantities. assumed to be driven by parallel streaming along stochastic magnetic field. Recently, research on convection by electrostatic fluctuations has been initiated theoretically and experimentally. These electrostatic and magnetic fluctuation contributions to transport can be obtained from the drift kinetic equation. The mean (ensemble-averaged) distribution function, $\langle f \rangle$, evolves as

$$\partial \langle f \rangle / \partial t = - [(\tilde{E} \times \langle \underline{B} \rangle / \langle B \rangle^2) + v_{\parallel} \tilde{\underline{B}}] \cdot \nabla \tilde{f} , \qquad (1)$$

where the tilde is used to denote the fluctuating fields and distribution function. The time evolution of a plasma quantity $\langle R(r,t) \rangle = \int R(v) \langle f \rangle dv$, due to radial transport, is given by

$$\partial \langle R \rangle / \partial t = (1/r) \int d\underline{v} \; R(\underline{v}) \partial / \partial r \{ [(\tilde{\underline{E}} \times \langle \underline{B} \rangle / \langle B \rangle^2 \cdot \hat{r} + v_{\parallel} \tilde{B}_r] r \tilde{f} \} , \qquad (2)$$

where we assumed that $\langle B \rangle$ is slowly varying in space (compared to the fluctuations) and $\tilde{E}$ is electrostatic. We can now identify the radial flux of $\langle R \rangle$ as

$$\Gamma_R = \int dv \; R(v) \; [(\tilde{\underline{E}} \times \langle \underline{B} \rangle / \langle B \rangle^2) \cdot \hat{r} + v_{\parallel} \tilde{B}_r] \tilde{f} . \qquad (3)$$

Taking $R(v) = 1_{\perp}$ we see that particle flux from electrostatic fluctuations is related to $\langle \tilde{n} \tilde{E} \rangle$, and from magnetic fluctuations to $\langle \tilde{j}_{\parallel} \tilde{B}_r \rangle$, where $j_{\parallel}$ fluctuating current density parallel to $\langle B \rangle$ and $\tilde{E}$ represents the fluctuating electric field perpendicular to $\langle B \rangle$. The radial flux of field-aligned current (a possible dynamo contribution) is obtained by taking $R(v) = \underline{v}_{\parallel}$. We see that $\Gamma_{v_{\parallel}}$ is determined by $\langle \tilde{j}_{\parallel} \tilde{E} \rangle$ for electrostatic fluctuations and $\langle \tilde{p} \tilde{B}_r \rangle$ for magnetic fluctuations, where the fluctuation in the parallel pressure is $\int v_{\parallel}^2 \tilde{f}(\underline{v}) d\underline{v}$. The energy flux, obtained from taking $R(v) = v^2$, has an electrostatic contribution given by $\langle \tilde{p} \tilde{E} \rangle_{\perp}$ where $\tilde{p}$ is the pressure fluctuation. The magnetic contribution is determined by $\langle \tilde{Q}_{\parallel} \tilde{B}_r \rangle$, where $\tilde{Q}_{\parallel}$ is the fluctuation in the parallel heat flux, given by a third velocity moment of the distribution function, $\tilde{Q}_{\parallel} = \int v_{\parallel} v^2 \tilde{f} dv$. The above quadratic quantities are listed, for later reference, in the first two columns of Table II.

A caveat, particularly relevent to present RFP experiments, is that we have considered the parallel electron drift speed, and its fluctuations, to be small. Considering the drift to be nonzero, the energy flux from electrostatic fluctuations becomes

$$\Gamma_E = \langle \tilde{p} \tilde{E} \rangle + v_d^2 \langle \tilde{n} \tilde{E} \rangle + 2 n v_d \langle \tilde{v}_d \tilde{E} \rangle + n \langle \tilde{v}_d^2 \tilde{E} \rangle + 2 v_d \langle \tilde{n} \tilde{v}_d \tilde{E} \rangle + \langle \tilde{v}_d^2 \tilde{n} \tilde{E} \rangle$$

where v_d is the electron drift speed. The last three higher order terms on the right side can be ignored if the fluctuations are small. The second and third terms are small if the equilbrium electron drift is small compared to the thermal speed (i.e., small streaming parameter). The current transport from magnetic fluctuations is similarly modified.

Additional transport arises from MHD effects not captured in the above quadratic terms. Fluctuating fluid flow gives rise to convective particle flux given by $\langle \tilde{n}\tilde{u}_r \rangle$ and energy flux given by $(5/2)T\langle \tilde{n}\tilde{u}_r \rangle$, where $\tilde{u}_r$ is the radial fluid velocity (primarily composed of the ion flow velocity). The fluctuating flow also produces an electric field given by $\langle \tilde{u} \times \tilde{B} \rangle$. This electric field drives parallel current in the plasma and is the basis for the MHD dynamo. These MHD contributions to transport are listed in the third column of Table II.

Table II. Quadratic quantities which determine particle, parallel current, and energy transport from electrostatic, magnetic, and MHD fluctuations. It is assumed that the streaming parameter is small.

	Electrostatic Fluctuations	Magnetic Fluctuations	MHD Fluctuations
Particle Transport	$\langle \tilde{n}\tilde{E} \rangle$	$\langle \tilde{j}_n \tilde{B}_r \rangle$	$\langle \tilde{n}\tilde{u}_r \rangle$
Parallel Current Transport	$\langle \tilde{j}_n \tilde{E} \rangle$	$\langle \tilde{p}_n \tilde{B}_r \rangle$	$\langle \tilde{u} \times \tilde{B} \rangle$
Energy Transport	$\langle \tilde{p}\tilde{E} \rangle$	$\langle \tilde{Q}_n \tilde{B}_r \rangle$	

MAGNETIC FLUCTUATIONS AND MHD

It has long been known that the low frequency (< 30 kHz) magnetic fluctuations observed in the RFP agree with predictions for nonlinear tearing mode fluctuations, as calculated from various 3D resistive MHD computations. In both experiment (Hutchinson et al.), and computation (Schnack et al.,1985; Holmes et al., 1988; Nebel et al., 1989), the dominant Fourier modes measured at the edge have poloidal mode number m=1 and a range of toroidal mode numbers, n, peaked at that which yield a resonance close to the center. The modes are resonant within the reversal surface, but are global and nonzero over the entire cross-section. Edge measurements in MST indicate low frequency m and n spectra (shown in figure 2) quite similar to that observed in smaller devices. The computational spectra (Fig. 3) for a similar aspect ratio as MST are nearly identical to experimental spectra at low frequency (Fig. 2), with the exception that the experimental spread in n exceeds that of the code. The difference might be attributable to the Lundquist number S, the ratio of the resistive diffusion time to the Alfven transit time. The larger S of the experiment ($\approx 10^6$ vs 3×10^6 in the code) yield greater nonlinear mode coupling.

The Lundquist number increases with current in the RFP. The scaling of fluctuations with S is an important question which is not yet resolved theoretically. Aproximate nonlinear turbulence analyses for either tearing fluctuations (Strauss, 1986) or resistive interchange fluctuations (Hender and Robinson, 1983) yield $\tilde{B}_r$ scaling as inverse fractional powers of S, whereas recent numerical studies over a limited range of S values predict $\tilde{B}_r$ independent of S (An et al., 1987; Nebel et al., 1989). A limited S scan in OHTE yielded an $S^{-1/2}$ dependence (LaHaye et al., 1984). In MST, it is seen that the low frequency fluctuations also tend to decrease with plasma current, although a correlation with S is not observed.

Internal diagnosis of magnetic fluctuations is scant relative to the spectral analyses at the edge. Nonetheless, radial profile measurements of magnetic fluctuations at low current in OHTE (LaHaye et al.,1984) and HBTX-IA (Brotherton-Ratcliffe, et al., 1987) have been reported to agree with linear MHD eigenfuctions for tearing modes. It is now known that the nonlinear mode structure produced from computation is indeed similar.

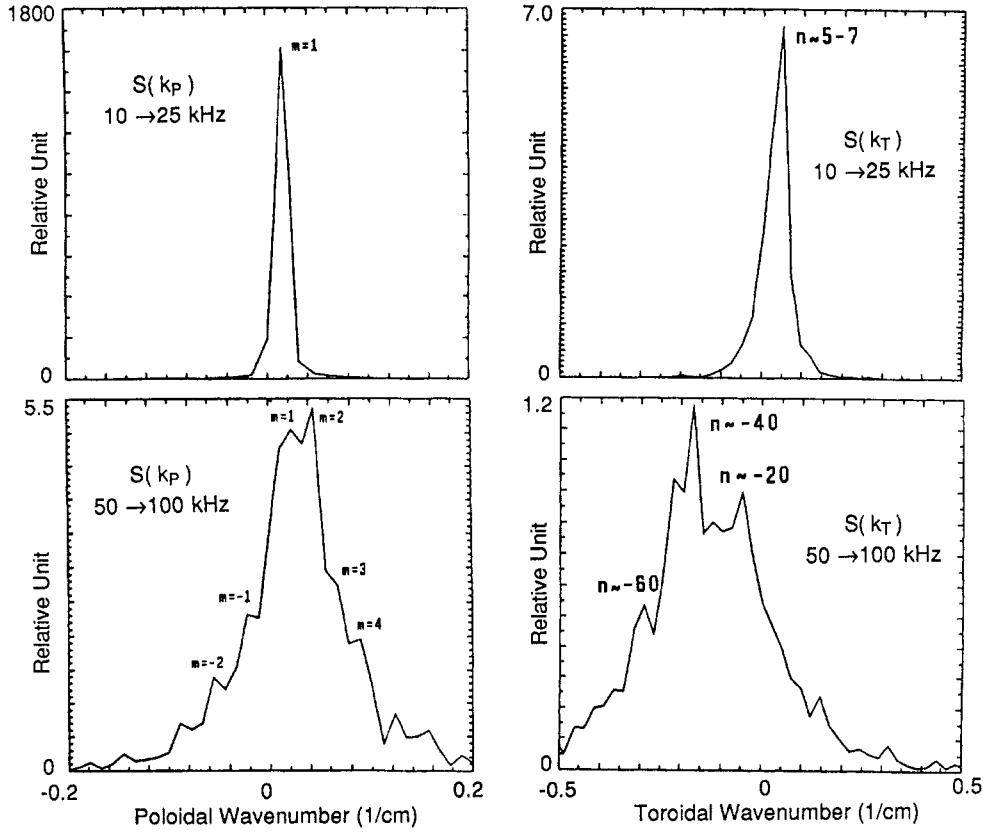

Fig. 2. Poloidal and toroidal mode number spectra of magnetic fluctuations in MST at low frequency and high frequency. From 2-pt phase shift measurements. R/a = 3.

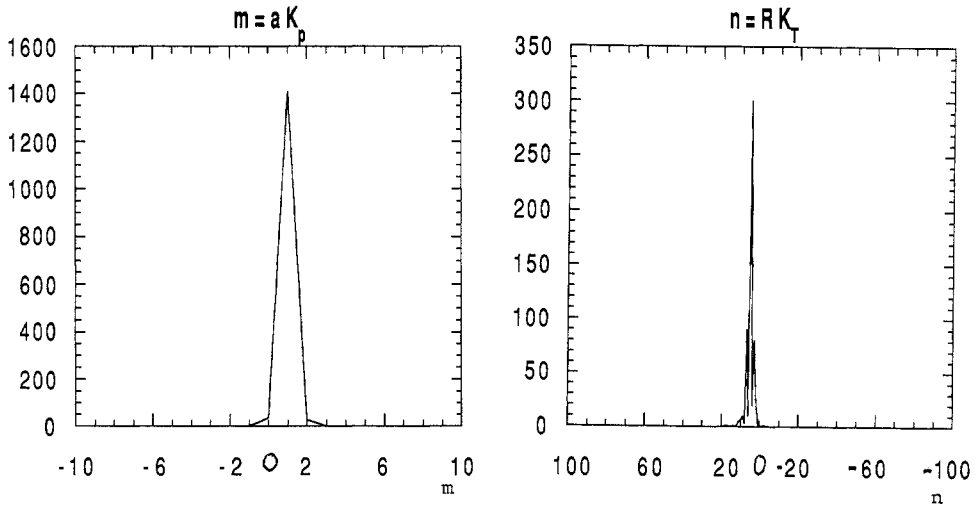

Fig. 3. Poloidal and toroidal mode number spectra of magnetic fluctuations, from 3D MHD computation. $S = 6 \times 10^3$, R/a = 2.5. Vertical axes are arbitrary units.

MHD also predicts the occurence of pressure-driven resistive interchange fluctuations. In experiments, the pressure gradients appear to be largest in the outer part of the plasma. Thus, resistive interchange fluctuations might be expected to arise in the vicinity of the reversal surface and beyond. To maintain resonance with the equilibrium field in this low q region, the fluctuations would possess high toroidal mode numbers with consequently high frequency. Indeed, in experiments the mode numbers rise with frequency. In figure 2 we display the m and n spectra for MST for the frequency band between 50 kHz and 100 kHz. Both the mean mode numbers and width of the distribution increase with frequency. An interesting feature is that the mean n number reverses sign from low to high frequency, consistent with the resonant surfaces shifting from inside to outside reversal as frequency increases. The theoretical study of resistive interchange modes is less well-developed than for the more global tearing modes. Predictions for the mode spectra are not yet available. Investigation of these pressure-driven fluctuations is critical in order to predict the beta achievable in RFPs.

TRANSPORT BY MAGNETIC FLUCTUATIONS

The RFP transport process which has recieved the most attention is the transport of field-aligned-current. Current transport is implicit in the experimental observation of the persistence of field reversal for times longer than permitted by classical resistive diffusion (Caramana and Baker, 1984). There are two mechanisms, listed in Table II, by which j is transported radially by magnetic fluctuations. In the MHD dynamo, current is driven, and thus "transported", by the fluctuation-induced electric field $\langle \tilde{u} \times \tilde{B} \rangle$. The parallel component of this term has been shown to be expressible in a diffusive form given by $\nabla\cdot[D\nabla(J/B)]$, where D is the effective transport coefficient, sometimes called the hyper-resistivity (Strauss, 1985,1986; Boozer, 1986; Bhattacharjee and Hameiri, 1986). The MHD dynamo model is established through self-consistent computation (Aydemir and Barnes, 1984; Strauss, 1984; Caramana and Schnack, 1986; Dahlburg, et al., 1988), and is consistent with analytical quasilinear calculations (Hameiri and Bhattacharji, 1987). It is compatible with the view of relaxation through resistive reconnection to the minimum energy "Taylor" state (Taylor, 1974). This MHD scenario is amply documented in the literature. It is buttressed by agreement with measured edge magnetic fluctuation spectra.

In both experiment and MHD computation, the dynamo field generation can be manifest as either continuous field generation accompanied by continuous broadband magnetic fluctuations, or by discrete dynamo events associated with the sudden appearance of m=0 and m=1 modes. The former case is the typical one. However, under certain conditions the toroidal magnetic field at the wall, $B_T(a)$ is observed to have a sawtooth time dependence, with $B_T(a)$ decreasing in time only during the sawtooth crash. These have been carefully studied in ZT40M (Watt and Nebel, 1983; Wurden, 1984; Watt and Little, 1984). Thus, the sawtooth crash is interpreted as discrete dynamo events. Sawteeth in RFPs were predicted by computational investigations of reconnection (Caramana et al., 1983). In figure 4 we display sawteeth in MST (Almagri et al., 1989; Prager et al., 1990). Sawteeth produced recently by a 3D nonlinear, resistive MHD computation (Kusano and Sato, 1989) are displayed in fig. 5. For low aspect ratio (fig. 5a) the code results for $B_T(a)$ resemble the experiment. The code predicts that the crash is accompanied by modes with m = 1 and n ≈ 2R/a. In MST, with R/a = 3, precursor oscillations are observed with m = 1, n ≈ 6. In ZT40M, in which R/a is nearly twice that of MST, precursors occur with n between 8 and 15. It is interesting to note that sawtooth activity in MST is generally more prevalent than in devices with larger aspect ratio. In MST, sawteeth can be produced at all values of pinch parameter (a dimensionless measure of the plasma current), whereas in ZT40M they occur dominantly at high pinch parameter. This trend is observed in the computation. As aspect ratio is increased the sawteeth subside and the reversal is generated continuously (fig. 5b). Presumably, at low R/a values the modes are widely separated in wavelength ($n=RB_p/aB_T$ for m=1) and grow to large amplitude, with little nonlinear interactions, until the discrete dynamo event occurs.

An alternative dynamo mechanism might occur through free streaming of electrons along the fluctuating magnetic field. This effect is completely distinct from the

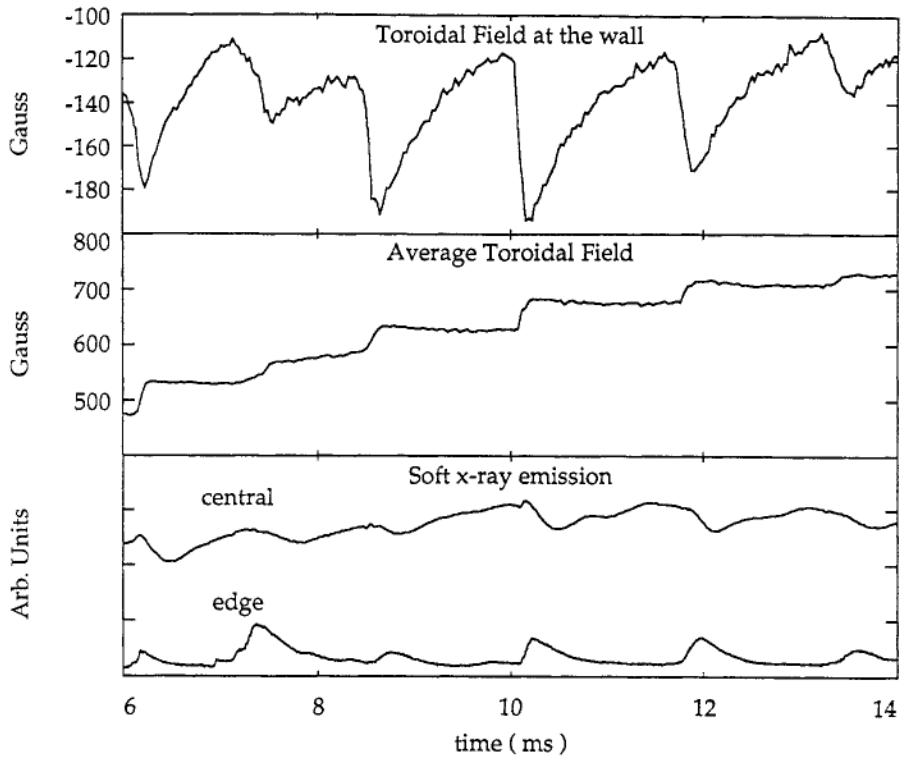

Fig. 4. Sawtooth oscillations in MST

$\langle \tilde{u} \times \tilde{B} \rangle$ effect of MHD (except, of course, that the magnetic fluctuations themselves can be an MHD effect). It is represented in the second term in equations (1)-(3) and the middle entry of TABLE II. This approach to current transport is known as the "kinetic dynamo" (Jacobson and Moses, 1984). The model predicts reversal if a pre-determined stochastic magnetic field is assumed and transport is given by the Rechester-Rosenbluth expression. A recent calculation employing drift-Alfven turbulence includes the self-consistent effect of the streaming particles on the magnetic field through the imposition of Ampere's law and quasi-neutrality (Terry and Diamond, 1990). It was found that with the imposed self-consistency constraints, the transport of field-aligned current by this mechanism is small. It is seen from Table II that this transport is proportional to $\langle \tilde{p}_{\parallel} \tilde{B}_r \rangle$. The coherent part of the fluctuations, in which the presure fluctuation at a given k is proportional to the field fluctuation at the same k, i.e., $\tilde{p}(k) \sim \tilde{B}_r(k)$, yields flutter diffusion (the Rechester-Rosenbluth term). However, this effect is cancelled by the incoherent part of $\tilde{p}$ which includes coupling of pressure and field fluctuations at different k values.

Recent experimental observation of fast electrons in the edge of ZT40M (Ingraham et al., 1990) are compatible with the kinetic dynamo model. A population of electrons, with density several percent of the total, exists with a half-Maxellian velocity distribution and a temperature roughly twice that of bulk electrons at the center and ten times that of the bulk at the edge. These observations appear to be compatible with electrons originating at the center and travelling to the edge, accelerated by the applied electric field within the reversal surface. Energetic electrons have been observed in many devices, most recently in TPE-1RM15 (Yagi et al., 1990). Perhaps the most intriguing observation in ZT40M is that the current carried by these electrons is comparble to the total current at the edge. These observations are consistent with central electrons accelerated from the center by the applied electric field. Actually, the occurrence of these fast electrons at

the edge is not incompatible with the self-consistent calculation since fast electrons stream through the wave fields and, on average, do not interact with the waves.

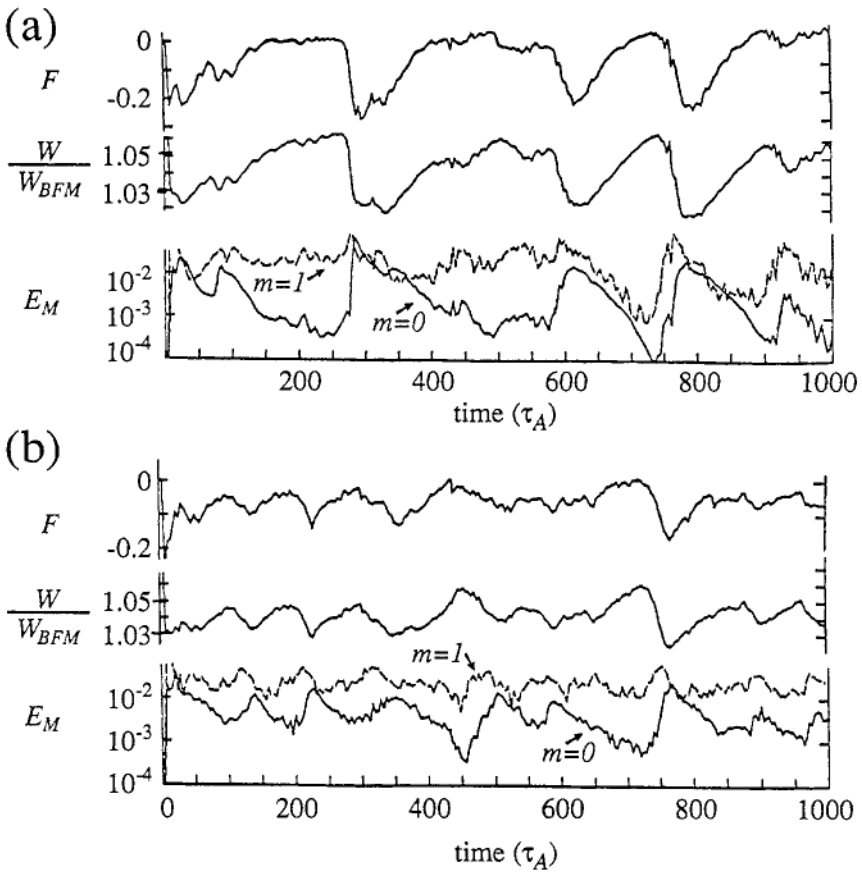

Fig. 5. Sawtooth oscillation from MHD computation at an aspect ration of (a)1.6 and (b)4.8. (From Kusano and Sato, 1989).

It is anticipated that in larger devices, with lower applied electric field, the fast electrons will be absent. Indeed, preliminary measurements with an xray target probe in MST do not reveal the presence of fast electrons. In ZT40M, as well, the fast electron temperature is observed to increase with applied electric field. In the MST case, the self-consistency requirements should constrain the bulk. However, the experimental absence of fast electrons does not disprove the kinetic dynamo effect, since the bulk electrons might still be free-streaming.

At this point, neither dynamo model is experimentally validated, although the self-consistent MHD dynamo is on a firmer theoretical basis. Perhaps the question will persist until a measurement of the relevant quadratic quantities is accomplished. That is, the relative importance of the kinetic and MHD dynamo effects can be assessed by measuring $\langle \tilde{p}_{\shortparallel} \tilde{B}_r \rangle$ and $\langle \underline{\tilde{u}} \times \underline{\tilde{B}} \rangle$ in the edge.

In view of this unsettled dynamo issue, it is ironic that the conventional view of RFP energy and particle confinement is that it is limited by transport along a stochastic magnetic field. In this model, the tearing modes stochasticize the magnetic field over the portion of the plasma for which the modes are resonant,

which corresponds to a majority of the region within the reversal surface. Confinement is thus poor within this core region. The surfaces are intact in the outer, nonresonant portion of the plasma, as indicated from puncture plots produced from tearing computations (Caramana and Schnack, 1986). This outer region is then the dominant confinement region. The pressure profile is relatively flat in the core, with the gradients localized to the edge. Such a pressure profile appears to be somewhat consistent with experimental indications, although complete profile measurements have not yet been obtained. In the edge, resistive interchange modes would then arise and ultimately determine the confinement and beta limit. This picture is consistent with spectral measurements of magnetic fluctuations. Moreover, in most RFPs, including recent results from MST, the global energy confinement is of the order of the Rechester-Rosenbluth estimate obtained from the edge magnetic fluctuations and the parallel correlation length of order of the minor radius, as recently indicated from edge measurements in ZT40M (Miller, 1990). These inferences are extremely coarse, and further work requires measurement of $\langle \tilde{j}_{\parallel} \tilde{B}_r \rangle$ to obtain the particle transport and, ideally, $\langle \tilde{Q}_{\parallel} \tilde{B}_r \rangle$ to obtain the energy transport, as indicated in TABLE II.

A final anomolous feature of energy flow in RFP experiments, although perhaps an attractive one, is that the ions are somentimes heated at a rate far greater than can be explained by collisional transfer from electrons which receive the Ohmic heating power (Howell and Nagayama, 1985; Ogawa and Maejima,1985; Carolan et al., 1987; Wurden et al., 1088; Cararro et al.,1990). In fact, in many experiments it has been observed that the ions are hotter than the electrons (most recently observed in MST under certain conditions). In past experiments in HBTX it had been observed that the anomalous ion heating is strongest for situations in which the magnetic fluctuations are largest (Carolan et al., 1988). In recent HBTX experiments the independence of the ion anomaly to Ohmic heating was further demonstrated by altering the Ohmic heating through laser ablation (Carolan et al., 1990). Laser ablation is used to inject impurities which enhance the Spitzer resistivity and the loop voltage. Nevertheless, the ion temperature was unaffected. This is in contrast to alterations of the loop voltage through techniques which affect the plasma fluctuations.

There is a belief that the ions are heated by viscous dissipation of fluid velocity fluctuations associated with tearing mode fluctuations. Quantitative theoretical or computational demonstration of this effect is a topic of current research.

ELECTROSTATIC FLUCTUATIONS AND TRANSPORT

The concentration upon MHD fluctuations has been at the relative neglect of electrostatic fluctuations. This has been motivated by the large magnetic fluctuations observed in experiment and the inherently magnetic nature of the dynamo effect. However, there is no a priori reason to assume that fluctuations in electric potential and other quantities are more benign than, say, in a tokamak. Such fluctuations can have a non-MHD origin, such as the plethora of drift wave instabilities, or can accompany MHD fluctuations such as resistive interchange.

Recently, edge Langmuir probe measurements of electrostatic fluctuations have commenced on MST (Prager et al., 1989), REPUTE (Toyama and Ji, 1990), and ZT40M (Miller et al, 1990). As in a tokamak, the fluctuations are large (several tens of percent) and decrease monotonically with frequency. The results reported here are still preliminary. Fluctuations have not yet been sampled at many locations at the plasma edge and the presence of fast electrons in some experiments complicates the analysis. Most importantly, it appears that the temperature fluctuations are large, between tens of percent, which is greater than observed in tokamaks (Lin et al., 1989). Thus, temperature fluctuations must be carefully included in the analysis of the Langmuir probe data.

The particle convection from $\langle \tilde{n}\tilde{E} \rangle$ is significant in ZT40M and of order of the actual particle flux at the edge. In REPUTE probes have been inserted to a minor radius of one-half the plasma radius ($r = a/2$). The plasmas investigated were greatly derated for probe insertion, resulting in an electron temperature of 25 eV to 30 eV at $r = a/2$. They find that the convective energy flux from density fluctuations (from $T\langle \tilde{n}\tilde{E} \rangle$) is very small, and roughly equal and opposite to

conductive transport from temperature fluctuations (from $n\langle\tilde{T}\tilde{E}\rangle$), as indicated in Fig. 6. Another curious result of their study is that the parallel and

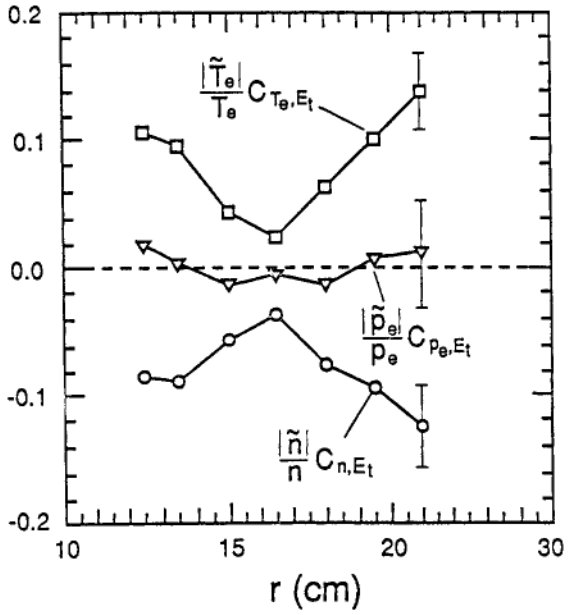

Fig. 6. Electrostatic transport in REPUTE from density and temperature fluctuations. C(a,b) is the correlation between a and b.

perpendicular wavenumbers are about equal ($k_{\parallel} \approx k_{\perp}$). This is in opposition to the expectation that $k_{\parallel} << k_{\perp}$, as is true in tokamaks and applies to most turblence models. Electrostatic fluctuations will require continued effort in several devices, in order to evolve a reliable picture.

MAJOR ISSUES AND NEXT STEPS

The RFP as a reactor concept (Bodin et al., 1986; Conn et al., 1988) confronts three major physics issues: confinement, the electrical boundary condition, and current drive. Their status is summarized below.

Confinement: The physics of confinement will require a detailed investigation of the correlation of fluctuations with transport. However, in a programatic sense, the major next step is to test confinement at high current and large size. Two simple experimental observations form the basis for a favorable confinement scaling for the RFP. First, all RFPs operated to date have beta values of the order of 10% or greater, where beta is the ratio of the volume averaged pressure to the surface magnetic field. Second, the plasma resistance scales classically. From these two premises (taking β = 10%) follows the scaling law $\tau_E \sim a^2 I^3/N^{3/2}$, where N is the line density, $n\pi a^2$. Naturally, all past experiments obey this relation. At moderate current, the confinement time of MST (≈1.5 ms) is about one half of that anticipated from the scaling relation. At high current, it is further below the expectation. At present, MST is in a phase of evolving parameters as the plasma control systems (such as field error control and voltage programming capabilities) evolve. This scaling relation would yield confinement times in RFX (Malesani, 1987) and ZTH (Dreicer, 1987) of 20 ms and 40 ms, respectively. Thus, a clear experimental program is in place to test the scaling conjecture, i.e., to test whether beta remains at the 10% level at large current and size. Like most scaling relations, the constant beta scaling does not possess a firm theoretical

foundation. It is expected to be compatible with beta limitation from resistive interchange turbulence, a view expressed in scale invariance arguments (Connor and Taylor, 1984) and nonlinear turbulence theory assuming Rechester-Rosenbluth transport (Hender and Robinson, 1983; Carreras and Diamond, 1989).

The three new RFP devices, MST (now operating), RFX (under construction) and ZTH (under construction) form a complementary set of experiments to test RFP confinement. Although roughly the same size, RFX and ZTH both have roughly ten times the volt-second capability of MST. This accounts for the longer duration and higher currents, as depicted in Table III. The initial operation of MST has produced plasma current up to 0.6 MA and plasma duration (at somewhat lower current) of up to 80 ms (with a flat-top period of 25 ms). The relatively low startup voltage (< 150V) and sustainment voltage (15V at 0.4 MA) virtually assures that RFX and ZTH will attain their design current and plasma duration. At a fixed current value, the electron pressure is about constant, i.e., density and electron temperature vary inversely (ion temperature has not been yet measured during a density scan). Central density is variable from about 3×10^{13} cm^{-3} to 7.5×10^{12} cm^{-3}, while temperature varies from 0.4 keV down to less than 100 eV. Beta is about 10% at low current (≈ 200 kA) falling to about 5 % at 500 kA. As in some other RFPs (Bodin, 1987), the rate of fall decreases at high current. A major concern is whether the decline with beta is intrinsic to RFP confinement or a feature of early operation of MST. The present MST parameters represent a minimum set of parameters, rather than an optimized set.

Table III Plasma parameters for the existing data base, MST, RFX, and ZTH

	a(m)	R(m)	I(mA)	Duration (s)	τ_E(ms)	S
Existing Database (typical)	~0.2	~1	~0.3	0.01-0.03	0.1-0.7	$<10^6$
MST	0.5	1.5	0.6 (1 Proj)	0.08	1.5(~5 Proj)	$<10^7$
RFX	0.46	2	2	0.25	20	$<7 \times 10^7$
ZTH	0.4	2.4	2-4	0.4	20-40	mid-10^8

Electrical Boundary Condition: Most RFP experiments have operated with close-fitting conducting shells. In nonlinear MHD computation, removal of the close-fitting shell results in growth of the dynamo tearing modes which deepen reversal (Ho et al., 1989). However, the modes also produce a central fluctuation-induced electric field in a direction to suppress the plasma current. To maintain the current then requires an enhanced loop voltage. Recent experiments in HBTX-1C with a resistive shell are in good qualitative agreement with these predictions (Alper et al., 1989); magnetic fluctuations and loop voltage grow in time eventually terminating the discharge prematurely. On the other hand, resistive shell experiments in OHTE display only bursts of magnetic activity and the plasma can persist for many resistive shell penetration times (LaHaye et al., 1988). There is a conjecture (Nebel, 1990) that a relevant distinction between the two experiments is the parameter $\omega^* \tau_s$, which compares the electrical penetration time of the shell to the (inverse) diamagnetic drift frequency. This parameter is larger in OHTE than in HBTX-1C. The shell issue should be definitively settled in RFX and ZTH. RFX is built with a thick conducting shell and ZTH with a thin resistive shell (but with $\omega^* \tau_s >> 1$).

MHD computational study of feedback stabilization is also underway (Nilles et al., 1989). Results indicate that feedback at the boundary of a few dominant Fourier modes is sufficient to reduce the loop voltage to a value only modestly larger than that obtained with a conducting shell.

Current Drive: The major current drive scheme envisioned for an RFP is helicity injection through oscillations in the surface toroidal and poloidal voltages (Bevir

and Gray, 1980; Schoenberg et al., 1984). In past current drive tests in ZT40M the plasma was too resistive to produce a current drive effect greater than about 5% (Schoenberg et al., 1987). Thus, a definitive proof of principle test awaits the production of less resistive plasmas. Provision exists in the MST and ZTH designs for current drive tests after the attainment of appropriate plasma parameters.

SUMMARY

The RFP is an excellent vehicle to investigate turbulent fluctuations and associated transport of current (the dynamo effect), particles and energy. Many phenomena might be simultaneously active, including MHD flow effects, free-streaming along stochastic magnetic field, and electrostatic fluctuation effects. Diagnostics exist for a deeper experimental investigation into these phenomena, particularly through the measurement of key quadratic quantities. To examine the dominant physics issues for its reactor feasibility (confinement, shell effects, and current drive), the MST, RFX, and ZTH experiments form a complementary sequence of devices to test the physics and confinement conjectures upon which its reactor extrapolation is based.

ACKNOWLEDGEMENTS

Critical comments on the content of this work by P. Terry, S. Ortolani, and J. Sarff are much appreciated, as is the data provided by B. Alper, H. Toyoma, and P. Weber. This paper has benefitted greatly from input from the MST group, and has included data obtained by A. Almagri, S. Assadi, J. Beckstead, G. Chartas, D. Den Hartog, R. Dexter, S. Hokin, E. Nilles, T. Rempel, E. Scime, J. Sarff, C. Spragins, C. Sprott, and W. Shen.

This work is supported by the U.S. Department of Energy.

REFERENCES

Almagri, A.A. et al., (1989). Twelfth Int. Conf. on Plasma Physics and Controlled Nuclear Fusion Research, II, 757.
Alper, B. et al. (1989). Plasma Physics and Controlled Fusion, 31, 205.
An, Z.G. et al. (1987). Eleventh Int. Conf. on Plasma Physics and Controlled Nuclear Fusion Research, II, 663.
Aydemir A. and D.C. Barnes (1984). Phys. Rev. Lett., 52, 930.
Bevir, M. and J. Gray (1980). Proceedings of the Reversed Field Pinch Theory Workshop, Los Alamos.
Bhattacharjee, A. and E. Hameiri (1986). Phys. Rev. Lett., 57, 206.
Bodin, H.A.B.(1987). Physics of Mirrors, Reversed Field Pinches and Compact Tori, Proc. of the Course and Workshop, Varenna, Italy, I, 3.
Bodin, H.A.B., R.A. Krakowski, S. Ortolani (1986). Fusion Technology, 10, 307.
Boozer, A.H. (1986). J. Plasma Phys., 35, 133.
Brotherton-Ratcliffe, D., C.G. Gimblett, I.H. Hutchinson (1987). Plasma Physics and Controlled Fusion, 29, 161.
Caramana, E.J. and D.A. Baker (1984). Nuclear Fusion, 24, 423.
Caramana, E.J., R.A. Nebel, D.D. Sch nack (1983). Phys. Fluids, 26, 1305.
Caramana, E.J. and D.D. Schnack (1986). Phys. Fluids, 29, 3023.
Carreras, B. and Diamond, P.H. (1989). Phys. Fluids B, 1, 1011.
Carolan, P.G et al. (1987). 14th European Con. on Controlled Fusion and Plasma Physics, II, 469.
Carolan, P.G. et al.(1988). 15th European Conf. on Controlled Fusion and Plasma Heating, II, 577.
Carolan, P.G. et al. (1990). 17th European Conf. on Controlled Fusion and Plasma Heating, Amsterdam.
Carraro, L. et al. (1990). 17th European Conf. on Controlled Fusion and Plasma Heating, Amsterdam.
Conn, R. et al. (1989). Twelfth Int. Conf. on Plasma Physics and Controlled Nuclear Fusion Research, III, 315.

Connor, J.W. and Taylor, J.B. (1984). Nucl. Fusion, 27, 2676.
Dahlburg, J., D. Montgomery, G.D. Doolen, L. Turner (1988). J. Plasma Physics, 40, 39.
Dreicer, H. (1987). Physics of Mirrors, Reversed Field Pinches and Compact Tori, Proc. of the Course and Workshop, Varenna, Italy, I, 359 .
Hameiri, E. and A. Bhattacharjee (1987). Phys. Fluids, 30, 1743.
Hender, T.C. and D.C. Robinson (1983). Ninth Int. Conf. In Plasma Physics and Controlled Nuclear Fusion Research, Baltimore, USA, III, 417.
Ho, Y.L., Prager, S.C., D.D. Schnack (1989). Phys. Rev. Lett., 62, 1504.
Holmes, J.A., B.A. Carreras, P.H. Diamond, V.E. Lynch (1988). Phys. Fluids, 31, 1166.
Howell, R.B. and Y. Nagayama (1985). Phys. Fluids, 28, 743.
Ingraham, J.C. et al. (1990). Phys. Fluids B, 2, 143.
Jacobon, A.R. and R.W. Moses (1984). Phys. Rev. A, 29, 3335.
Kusano, K. and Sato, T. (1989). Submitted to Nucl. Fusion.
LaHaye, R. et al.(1984), Phys. Fluids, 27, 2576.
LaHaye, R. et al. (1988). Nuclear Fusion, 28,918.
Lin, H., R.D. Bengston, C.P. Ritz (1989). Fusion Research Center Report 334, University of Texas.
Malesani, G (1987). Physics of Mirrors, Reversed Field Pinches and Compact Tori, Proc. of the Course and Workshop, Varenna, Italy, I,331 .
Miller, G. (1990). U.S.-Japan Workshop on Fluctuations in RFP/ULQ Plasmas, Madison, Wisconsin.
Nebel, R.A., E.J. Caramana, D.D. Schnack (1989). Phys.Fluids B, 1, 1671.
Nebel, R.A. (1990). private communication.
Nilles, E.J., S.S. Prager, Y.L.Ho (1989). Bull. Am. Phys. Soc., 34, 2147.
Ogawa, K. and Y. Maejima (1985). Nucl. Fusion, 25, 1295.
Prager, S.C. et al. (1990). Phys. Fluids B, 2, 1367.
Rechester, A.B. and M.N. Rosenbluth (1978). Phys. Rev. Lett.,40, 38.
Schnack,D.D., E.J. Caramana and R.A. Nebel (1985). Phys. Fluids, 28, 321.
Schoenberg, K.F., R.F. Gribble, D.A. Baker (19840. J. Appl. Phys., 56, 2519.
Schoenberg, K.F. (1987). 11th Int. Conf. on Plasma Physics and Controlled Nuclear Fusion Research, II, 423.
Strauss, H.R. (1984). Phys. Fluids, 27, 2580.
Strauss, H.R. (1985). Phys. Fluids, 28, 2786.
Strauss, H.R. (1986). Phys. Fluids, 29, 3008.
Taylor, J.B. (1974). Phys. Rev. Lett., 33, 1139.
Terry, P.W. and P.H. Diamond (1990). Phys. Fluids B, 2, 1128.
Toyama, H. and H. Ji (1990). Transport Task Force Workshop, Hilton Head, South Carolina.
Watt, R.G. and E.M. Little (1984). Phys. Fluids, 27, 784.
Watt, R.G. and R.A. Nebel (1983). Phys. Fluids, 26, 1168.
Wurden, G.A. (1984). Phys. Fluids, 27, 551.
Wurden G.A. et al. (1988). 15th European Conf. on Controlled Fusion and Plasma Plasma Physics, II, 533.
Yagi, Y., et al. (1990). 17th European Conf. on Controlled Fusion and Plasma Heating, Amsterdam.